

Separation of Spin and Charge Transport in Pristine π -Conjugated Polymers

Matthew Groesbeck¹,* Haoliang Liu¹,* Marzieh Kavand, Evan Lafalce, Jingying Wang, Xin Pan, Taniya Hansika Tennahewa¹, Henna Popli¹, Hans Malissa¹, Christoph Boehme¹, and Z. Valy Vardeny¹†
Department of Physics and Astronomy, University of Utah, Salt Lake City, Utah 84112, USA

 (Received 3 June 2019; revised manuscript received 4 October 2019; accepted 6 January 2020; published 14 February 2020)

We have experimentally tested whether spin-transport and charge-transport in pristine π -conjugated polymer films at room temperature occur via the same electronic processes. We have obtained the spin diffusion coefficient of several π -conjugated polymer films from the spin diffusion length measured by the technique of inverse spin Hall effect and the spin relaxation time measured by pulsed electrically detected magnetic resonance spectroscopy. The charge diffusion coefficient was obtained from the time-of-flight mobility measurements on the same films. We found that the spin diffusion coefficient is larger than the charge diffusion coefficient by about 1–2 orders of magnitude and conclude that spin and charge transports in disordered polymer films occur through different electronic processes.

DOI: [10.1103/PhysRevLett.124.067702](https://doi.org/10.1103/PhysRevLett.124.067702)

Organic semiconductors (OSECs) have been studied extensively, not only because of their versatility for electronic and optoelectronics applications such as organic light emitting diodes [1], transistors [2], and solar cells [3], but also for their potential applications in spintronics [4–8]. OSECs are predominantly made of light atoms with low atomic numbers and, therefore, the electronic states in OSECs typically exhibit weak spin-orbit coupling (SOC), which may lead to long spin relaxation times. This suggests potential applications as spin transport materials in spintronics devices [9,10]. Indeed, for more than a decade, OSECs have been demonstrated to work as efficient buffer layers in spin-valve structures in which they are sandwiched between two ferromagnetic (FM) electrodes with different coercivities [4,9,11] which serve as injector-detector pair of both a spin-polarized current as well as an electrical current under application of a bias voltage at cryogenic temperatures.

More recently, the transport of pure spin current (in the absence of charge current) through OSECs has been demonstrated using spin pumping via ferromagnetic resonance (FMR) excitation of a FM substrate at room temperature [12]. Here, the spin current in the OSEC layer is launched through scattering of FMR-induced magnons at the FM-organic interface, which serves as a spin transport layer. The detection of the pure spin current is possible through observation of the inverse spin Hall effect (ISHE), which is the SOC-induced electromotive force—detected by a voltage or current measurement—transverse to the pure spin [13]. Pure spin currents in OSEC layers have been demonstrated with the ISHE by using both nonmagnetic detector layers with strong SOC or directly through the low-SOC organic transport layers themselves [14–16]. The latter approach was first demonstrated by using a bilayer structure consisting of the ferrimagnetic insulator

$Y_3Fe_5O_{12}$, and the conducting polymer PEDOT:PSS [14], while the former has been accomplished using trilayer structures composed of a FM injector layer, an OSEC transport layer, and an ISHE detector layer with strong SOC, typically Pt or Pd. These trilayer structures have been used to obtain spin diffusion lengths of various OSEC interlayers [17–21]. Importantly, using pure spin current and the ISHE for its detection circumvents a well-known problem of spintronics applications that rely on injection of spin-aligned carriers into the nonmagnetic layer, namely the impedance mismatch that occurs at spin-injector interfaces [22,23].

Charge transport in OSEC has been studied extensively in the past, and is generally considered to be well understood for most materials that fall into this class. Within disordered OSECs, such as π -conjugated polymers or small molecules, charge transport is governed by transitions between localized electronic states such as hopping or tunneling [24]. In contrast, spin-transport and spin-relaxation mechanisms in OSECs have been studied to a lesser degree. For localized electronic states various physical processes may affect both spin transport and spin relaxation, including interaction with nuclear spin states (hyperfine interaction) [25,26] and SOC [27,28]. For example, spin transport in the π -conjugated polymer poly(2,5-bis(3-alkylthiophen-2-yl)thieno[3,2-b]thiophene) (PBTtT) has been demonstrated to be governed by a SOC-mediated polaron hopping process [12]. Therefore, spin diffusion is expected to obey the diffusion length relation [29], $\lambda_S = \sqrt{DT_S}$, where λ_S is the spin diffusion length, D the charge carrier diffusion constant, and T_S is the spin-relaxation time. On the other hand, there are two theoretical models which predict that spin transport may be significantly more efficient than charge transport in OSEC films. One model claims that spin transport is mediated by

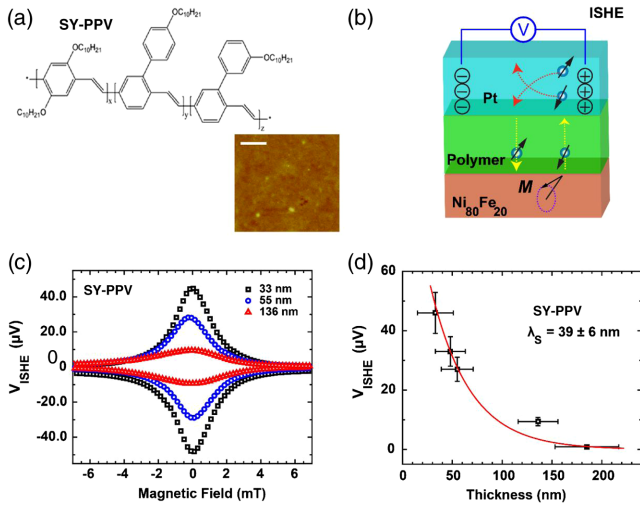


FIG. 1. Measurement of the spin diffusion length in the polymer SY-PPV using NiFe-polymer-Pt trilayer devices with various polymer thicknesses d in spin pumping or ISHE experiments. (a) SY-PPV molecular structure and surface morphology of ~ 150 nm thickness film deposited on Pt, measured by atomic force microscopy. The white scale bar corresponds to $4 \mu\text{m}$. (b) Schematics of the spin pumping process in the trilayer structure as explained in the text. (c) The ISHE voltage $V_{\text{ISHE}}(B)$ response generated in the Pt layer in trilayer devices with various d . (d) SY-PPV thickness dependence of the V_{ISHE} amplitude. The V_{ISHE} decay with d is modeled with an exponential function in order to extract the room temperature spin diffusion length λ_S in SY-PPV.

spin-exchange interaction at high carrier concentration [30]. The other model asserts that charge and spin transport may proceed in an impurity band that is effective in some domains of the film, where the spins interact via a long-range antiferromagnetic coupling that is more beneficial to spin transport. This is the so-called the two-fluids model [31].

In this letter, we report independent measurements of the spin diffusion length and the charge carrier diffusion length in a number of disordered π -conjugated polymer films, among which is a generic pristine polymer, namely, the Super Yellow poly-phenylene-vinylene (SY-PPV) [cf. Fig. 1(a)], is subjected to three different techniques: (i) spin pumping in FM-SY-PPV-Pt trilayers for ISHE measurements for obtaining the spin diffusion length, (ii) pulsed electrically detected magnetic resonance (EDMR) to obtain the transverse and longitudinal spin relaxation times, and (iii) time-of-flight experiments to obtain the charge carrier mobilities. The independent experimental verification of these critical spin- and charge-transport parameters allows us to establish whether or not spin transport and charge transport in SY-PPV are governed by the same physical mechanisms.

The spin diffusion lengths in polymer thin films were measured using NiFe-polymer-Pt trilayer devices with various polymer thicknesses, as depicted schematically

in Fig. 1(b). The various devices were fabricated on glass substrates each with 7 nm Pt evaporated film over 30 nm thick Cu contact pads, followed by the polymer spin transport layer, and capped with 15 nm Ni₈₀Fe₂₀ (NiFe) spin injection layer. The polymer spin transport layers were spin cast in an inert N₂ atmosphere with 2000–7000 rpm in order to obtain different thicknesses d , and the finished trilayer devices were protected from oxidation by depositing 100 nm SiO₂ capping layers. The surface morphology of the spin coated polymer films was characterized by atomic force microscopy, as shown in Fig. 1(a). The roughness was estimated to be ~ 3 nm for the SY-PPV thickness of ~ 150 nm; therefore, the magnetic properties of NiFe films deposited onto the various polymer films with different thicknesses are comparable. Additional details about the device structures and fabrication procedures can be found elsewhere [16,32]. For the ISHE measurements the devices were placed on a grounded coplanar waveguide. While the nonuniform B_1 field distribution generated by the coplanar waveguide prohibits determination of the absolute ISHE conversion strength [33], it does allow for the comparison of relative ISHE magnitudes, assuming the B_1 distribution is similar in all samples. Under FMR conditions, the FM NiFe film generates pure spin current at the NiFe-polymer interface which propagates into the polymer layer perpendicular to the interface. Once the spin current reaches the Pt detection layer on the opposite side of the device, it induces an ISHE current in the Pt film between the two Cu electrodes. The resulting ISHE voltage V_{ISHE} was measured as a function of the applied static magnetic field B_0 over both positive and negative polarities [cf. Fig. 1(c)] in order to corroborate that the observed magnetic resonant response was due to the ISHE.

In order to determine the spin relaxation time T_S (T_S being equivalent to T_1 in spin pumping applications, with external field B_0 in plane) of paramagnetic charge carriers in the SY-PPV polymer, we conducted pulsed EDMR spectroscopy using a Bruker Elexsys E580 pulse EPR spectrometer and an X-band Flexline MD5 resonator, following similar studies on other π -conjugated polymers [34,35]. For these experiments we use a bipolar injection thin-film device (an organic light emitting diode) [34].

The measurement of T_1 was done using an inversion recovery pulse sequence, where a π pulse is applied causing an inversion of the spin population in the device, which then is allowed to relax over time T [36,37]. As shown in Fig. 2(b), the amplitude of the electrically detected spin echo increases with increasing T , allowing T_1 to be extracted from the decay. The transverse relaxation time T_2 was also measured for the same device using a $\pi/2 - \tau - \pi - \tau - \pi/2$ pulse sequence, which is a standard Hahn-echo sequence extended by the $\pi/2$ detection pulse [38] [Fig. 2(c)]. In this sequence the spin-dependent current is recorded with variation of the separation time τ . T_2 is

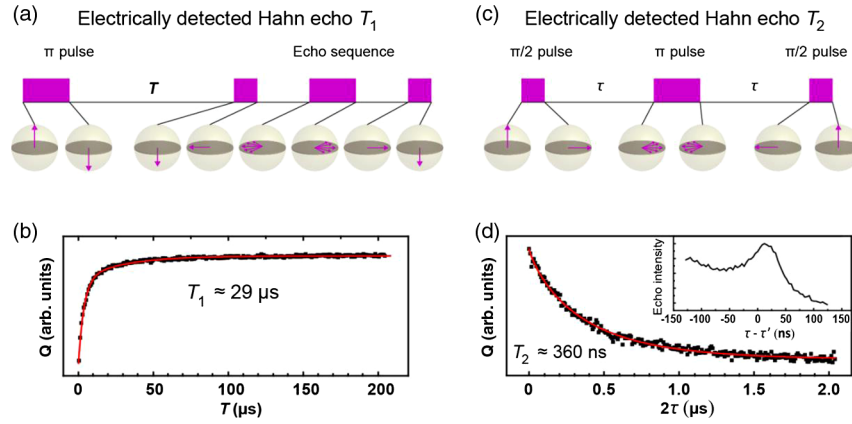


FIG. 2. Spin relaxation times in SY-PPV measured with EDMR spectroscopy. (a) Schematic of the electrically detected saturation recovery measurements. (b) Plot of the recovery signal amplitude as a function of saturation time T . (c) Schematic of the electrically detected Hahn-echo measurements, which deviate from inductively detected Hahn-echo sequences through the readout pulse which projects spin polarization onto the permutation symmetry operator that is probed in EDMR experiments [35]. (d) Plot of the Hahn-echo amplitude as a function of 2τ . Inset: A typical EDMR detected echo signal. By fitting the decays in (b) and (d), the spin relaxation times T_1 and T_2 are obtained, respectively.

again extracted from the spin echo decay with increasing τ , as shown in Fig. 2(d).

Time-of-flight measurements were carried out on devices consisting of ITO-PEDOT:PSS-polymers-Ca-Al stacks as shown in Fig. 3(a). Laterally, the devices had $2 \times 2 \text{ mm}^2$ large active areas, while the measured thickness of the polymer layer was $\sim 1 \mu\text{m}$. The laser pulses generate a thin layer of photoexcited species, including excitons and both positive and negative free carriers (polarons). By applying strong electric fields ($\sim 10^6 \text{ V/cm}$) we observed diffusion of photocarriers across the polymer film thickness. Under reverse bias conditions, holes were swept from the Ca to the ITO layer, while electrons were blocked at the Ca interface due to its high work function. Transit times were extracted from the transient photocurrent measurements, from which the zero-field mobility could be calculated.

Figure 1(c) shows $V_{\text{ISHE}}(B)$ measured in the Pt layer in the trilayer structure NiFe-SYPPV-Pt. The electric field direction is perpendicular to both the spin current and spin polarization directions [13], $\vec{E}_{\text{ISHE}} \propto \vec{J}_S \times \vec{\sigma}$, where \vec{J}_S and $\vec{\sigma}$ are the spin current and spin polarization, respectively. The data display a sign inversion of the voltage at fields B with negative polarity, which is a signature behavior of the ISHE, showing that pure spin transport occurs through the polymer layer. As shown in Fig. 1(c), $V_{\text{ISHE}}(B)$ decreases with increasing polymer film thickness d ; however, it is still significant at d beyond 150 nm, demonstrating that this polymer is quite efficient as a spin-transport medium. We exclude the possibility of contributions from magnetogalvanic effects, particularly the anisotropic magnetoresistance, in the NiFe layer due to the extremely high resistivity of the polymer spacer layer, found to be $\rho \sim 200 \Omega\text{m}$ [39]. The Pt detection layer, having resistance $R \sim 500 \Omega$, is essentially electrically isolated from any dc rectification voltage appearing across the NiFe layer. Figure 1(d) shows

that the amplitude of $V_{\text{ISHE}}(B)$ as a function of d is nicely described by an exponential decay [39], $V_{\text{ISHE}} \propto e^{-d/\lambda_S}$, where λ_S is the spin diffusion length of the SY-PPV polymer. From the fitting we obtain $\lambda_S = 39 \pm 6 \text{ nm}$ in SY-PPV.

The results of the spin echo measurements in SY-PPV film are shown in Fig. 2. The observed increase of the saturation recovery signal with increasing T , shown in Fig. 2(b), is well described by a double exponential decay, with time constants of 29 ± 1 and $3.8 \mu\text{s}$. The longer time constant is consistent with T_1 times in conjugated polymers [34], and the shorter time constant is ascribed to an additional short-lived, spin-dependent species. As previously explained, we take T_1 to be the relevant spin decay lifetime that governs the spin diffusion process in the polymer layer, although we note that T_2 may also have significant correlation with the charge diffusion rates in certain materials [43,44]. The decay of the T_2 spin echo response with increasing 2τ is shown in Fig. 2(d), and is fit nicely by a stretched exponential of the form $\exp(-\tau/T_2)^\beta$, which gives $T_2 = 361 \pm 7 \text{ ns}$ with $\beta = 0.85$.

Figure 3(b) shows the transient photocurrent $I_{\text{PC}}(t)$ of the time-of-flight measurements for a SY-PPV-based device with varying applied field strengths. Because of highly dispersive transport in the disordered polymer, $I_{\text{PC}}(t)$ follows a slow power-law decay, with a marked transition to a steeper decay once the initial excited carriers reach the other electrode [45]. The transition point or kink between the two power-law regions represents the transit time t_{tr} of the carriers across the film. From this kink in the $I_{\text{PC}}(t)$ decay the mobility μ can be calculated via the relationship $v_d = \mu F$, where v_d is the drift velocity and F the electric field, from which we obtain $\mu = L^2/t_{\text{tr}}V$, where L is the polymer layer thickness. The transit time t_{tr} is taken as the crossing point of the two power-law fittings, at the visible

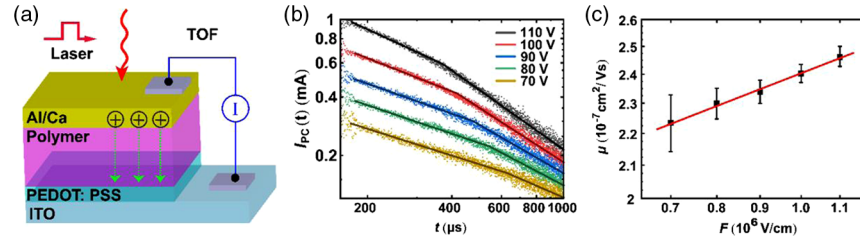


FIG. 3. Charge carrier mobility measurements in SY-PPV film using the time-of-flight (TOF) method. (a) Schematics of the TOF measurement. (b) TOF transient photocurrent decay I_{PC} with double logarithmic plots, showing typical dispersive transport in the film. The measurements were done at room temperature with effective electric fields of approximately 10^6 V/cm. (c) Electric bias field dependence of the TOF mobilities in SY-PPV. The solid line is fit by the Poole-Frenkel equation.

shoulder in the response curves. The transit time is shorter at higher applied voltage due to the Poole-Frenkel effect. Transit time versus applied field curves are shown for a SY-PPV film in Fig. 3(c), with fits to the Poole-Frenkel equation and relevant parameters given. The calculated zero-field mobility is $\mu(0) = 1.5 \pm 0.3 \times 10^{-7} \text{ cm}^2/\text{Vs}$. Based on the Einstein relationship the charge carrier diffusion coefficient $D_C = \mu k_B T / e$ can be estimated as $3.9 \pm 0.9 \times 10^{-9} \text{ cm}^2 \text{ s}^{-1}$ for SY-PPV, where k_B is the Boltzmann factor.

The parameters measured with the different experimental techniques are summarized in Table I. From the measured spin-relaxation time and spin diffusion length, we calculate the spin diffusion coefficient, $D_S = 5.2 \pm 1.6 \times 10^{-7} \text{ cm}^2 \text{ s}^{-1}$ using the relation $\lambda_S = \sqrt{D_S T_1}$. Also, from the carrier mobility measurement and the Einstein relationship, we derive the charge diffusion coefficient, $D_C = 3.9 \pm 0.9 \times 10^{-9} \text{ cm}^2 \text{ s}^{-1}$. It is thus clear that the spin diffusion coefficient in SY-PPV is more than 100 times larger compared to the charge diffusion coefficient. The spin density in SY-PPV, as determined by electron spin resonance [39], is comparable to the charge carrier density; thus we exclude the possibility of artificial higher spin density in SY-PPV due to defects or unintentional doping during the sample preparations. We note that while the determination of D_S from the diffusion length revealed $D_S/D_C \approx 135$, under the assumption that the longitudinal spin relaxation time T_1 determines the spin diffusion lengths [46–50], this disparity becomes even greater if T_2 determines the spin diffusion lengths, i.e., if the ISHE was dependent on spin coherence rather than (classical) spin polarization

memory [51]. We also measured the mobility of SY-PPV by I - V characteristics with the same device configuration (Pt-SYP-PV-NiFe) as the ISHE devices; the charge carrier mobility is one order larger than that obtained by time of flight [39], but the discrepancy still exists. This discrepancy between spin diffusion and charge diffusion is too large to be explained by simple experimental errors or uncertainties, and it is contrary to the recent finding that spin transport in doped polymers is mediated by polaron hopping, which would imply that spin transport would be due to the same mechanisms as charge transport [12].

To further verify the relation between spin and charge transport in disordered organic polymers, we also measured spin and charge transport in various polymers, as summarized in Table I. The corresponding spin diffusion lengths and mobility measurement results are shown in the Ref. [39]. Table I clearly demonstrates that there are always significant discrepancies between the spin and charge diffusion coefficients in disordered polymer films, in contrast to the comparable values of spin and charge diffusion coefficients in fullerene and its derivative. For the observed charge diffusion constants in disordered polymers, spin lifetimes of mobile charge carriers would need to exceed a few milliseconds [12] at room temperature to produce the observed spin diffusion lengths; therefore, charge diffusion as the origin of spin diffusion appears to be entirely unrealistic. We thus deduce that the separation of spin and charge transport is quite common in disordered polymer films, in contrast to other OSECs, such as fullerenes and its derivatives.

TABLE I. Summary of spin- and charge-transport parameters for different pristine polymer films.

Material	T_2 (ns)	T_1 (μs)	μ ($10^{-7} \text{ cm}^2 \text{ V}^{-1} \text{ s}^{-1}$)	N_c (10^{16} cm^{-3})	λ_S (nm)	D_C ($10^{-7} \text{ cm}^2 \text{ s}^{-1}$)	D_S ($10^{-7} \text{ cm}^2 \text{ s}^{-1}$)
SY-PPV	360 ± 7	29 ± 1	1.5 ± 0.1	0.7 ± 0.2	39 ± 6	0.04 ± 0.01	5.2 ± 1.6
P3HT	48 ± 5	~ 0.2	120 ± 8	1.2 ± 0.2	22 ± 5	3.08 ± 0.35	~ 240
Polyfluorene	253 ± 82 [34]	5 [34]	11 ± 2	...	118 ± 9	0.28 ± 0.02	278.5 ± 16.2
PC ₇₀ BM	...	~ 3.3 [52]	10000 ± 2000 [53] ^a	...	66 ± 8	257 ± 52	~ 132
C70	...	0.1–1 [54]	~ 6500 [55] ^a	0.10–3.12	17 ± 2	~ 167	29–290

^aThe mobilities of C70 and PC₇₀BM correspond to electrons; the mobility of holes is a few orders smaller [39].

Up to now, there have been two theories predicting spin transport without involving charge motion in disordered OSECs [30,31]. One is the exchange mediated spin diffusion model that suggests an additional exchange coupling mechanism for spin transport in organic media [30]. Polarons in OSEC films can be delocalized over ~ 1 nm length scale, and, at high concentrations ($> 10^{17}$ cm $^{-3}$), this may lead to an exchange interaction whereby carriers may transfer their spin alignment to adjacent sites (which may not be charged) without a physical hopping process. We note that this model has recently been experimentally verified by two different groups [46,56]. Therein, spin diffusion lengths measured by spin valve and lateral spin pumping in small molecule based materials and single crystal polymers were both shown to increase with increasing carrier densities. However, this model does not directly apply to our experimental results reported here, as direct exchange coupling cannot happen in pristine polymers with very low spin densities. We, therefore, also consider the two-fluids model that proposes antiferromagnetic coupling between the spins of localized carriers as the origin for spin transport [31]. There are similarities for the two theoretical models, as both assume that charge transport is related to charge carriers, but the difference is that spin transport proceeds through direct exchange coupling between spins of carriers in the exchange mediated spin diffusion model instead of a wave form that is deemed to be the origin in localized carriers with antiferromagnetic coupling for the two-fluids model. In our experiments, charge or spin densities are below the threshold of the exchange mediated spin diffusion model, and in addition, the disorder is much stronger in spin coated polymer films than in single crystals. Therefore, we conclude that the origin of spin-transport could possibly take place by a spin-wave propagation type mechanism. This is also consistent with a recent report of spin-information transfer through the overlap of wave functions [57].

In conclusion, we have studied spin and charge transport in disordered conjugated polymer films using three independent experimental techniques. These are spin pumping and ISHE measurements in trilayer devices of NiFe-polymer-Pt, pulsed EDMR spectroscopy, and time-of-flight and I - V response measurements. From these measurements we have extracted the room temperature spin and charge diffusion constants of the pristine polymers. We found that the spin diffusion constant is significantly larger than the charge diffusion constant, corroborating that the nature of spin and charge transport in disordered pristine polymer films are fundamentally different. We attribute the dominant spin-transport mechanism in disordered OSECs to the recently developed two-fluids model. These findings deepen our understanding of spin transport in disordered OSECs with strongly localized electronic states. Combined with recent reports of exchange

interaction dominant spin diffusion in highly doped polymers [45], we conclude that spin transport in π -conjugated polymers may proceed by wave propagation from antiferromagnetic coupling or direct spin-spin exchange interaction, separated from charge transport by hopping.

This work was supported by the National Science Foundation grant (DMR-1701427).

*These authors contributed equally to this work.

†Corresponding author.

val@physics.utah.edu

- [1] J. H. Burroughes, D. D. C. Bradley, A. R. Brown, R. N. Marks, K. Mackay, R. H. Friend, P. L. Burns, and A. B. Holmes, *Nature (London)* **347**, 539 (1990).
- [2] S. Kubatkin, A. Danilov, M. Hjort, J. Cornil, J.-L. Brédas, N. Stühr-hansen, P. Hedegård, and T. Bjørnholm, *Nature (London)* **425**, 698 (2003).
- [3] A. J. Heeger, *Adv. Mater.* **26**, 10 (2014).
- [4] Z. H. Xiong, D. Wu, Z. V. Vardeny, and J. Shi, *Nature (London)* **427**, 821 (2004).
- [5] V. A. Dediu, L. E. Hueso, I. Bergenti, and C. Taliani, *Nat. Mater.* **8**, 707 (2009).
- [6] C. Barraud, P. Seneor, R. Mattana, S. Fusil, K. Bouzehouane, C. Deranlot, P. Graziosi, L. Hueso, I. Bergenti, V. Dediu, F. Petroff, and A. Fert, *Nat. Phys.* **6**, 615 (2010).
- [7] M. Gobbi, A. Bedoya-Pinto, F. Golmar, R. Llopis, F. Casanova, and L. E. Hueso, *Appl. Phys. Lett.* **101**, 102404 (2012).
- [8] M. C. Wheeler, F. Al Ma'Mari, M. Rogers, F. J. Gonçalves, T. Moorsom, A. Brataas, R. Stamps, M. Ali, G. Burnell, B. J. Hickey, and O. Cespedes, *Nat. Commun.* **8**, 926 (2017).
- [9] M. Gobbi, F. Golmar, R. Llopis, F. Casanova, and L. E. Hueso, *Adv. Mater.* **23**, 1609 (2011).
- [10] H. Liu, J. Wang, M. Groesbeck, X. Pan, C. Zhang, and Z. Vardeny, *J. Mater. Chem. C* **6**, 3621 (2018).
- [11] V. Dediu, M. Murgia, F. C. Maticotta, C. Taliani, and S. Barbanera, *Solid State Commun.* **122**, 181 (2002).
- [12] S. Watanabe, K. Ando, K. Kang, S. Mooser, Y. Vaynzof, H. Kurebayashi, E. Saitoh, and H. Sirringhaus, *Nat. Phys.* **10**, 308 (2014).
- [13] E. Saitoh, M. Ueda, H. Miyajima, and G. Tatara, *Appl. Phys. Lett.* **88**, 182509 (2006).
- [14] K. Ando, S. Watanabe, S. Mooser, E. Saitoh, and H. Sirringhaus, *Nat. Mater.* **12**, 622 (2013).
- [15] Z. Qiu, M. Uruichi, D. Hou, K. Uchida, H. M. Yamamoto, and E. Saitoh, *AIP Adv.* **5**, 057167 (2015).
- [16] D. Sun, K. J. Van Schooten, M. Kavand, H. Malissa, C. Zhang, M. Groesbeck, C. Boehme, and Z. V. Vardeny, *Nat. Mater.* **15**, 863 (2016).
- [17] S. W. Jiang, S. Liu, P. Wang, Z. Z. Luan, X. D. Tao, H. F. Ding, and D. Wu, *Phys. Rev. Lett.* **115**, 086601 (2015).
- [18] M. Kimata, D. Nozaki, Y. Niimi, H. Tajima, and Y. C. Otani, *Phys. Rev. B* **91**, 224422 (2015).
- [19] Y. Tani, T. Kondo, Y. Teki, and E. Shikoh, *Appl. Phys. Lett.* **110**, 032403 (2017).

- [20] J. B. S. Mendes, O. Alves Santos, J. P. Gomes, H. S. Assis, J. F. Felix, R. L. Rodríguez-Suárez, S. M. Rezende, and A. Azevedo, *Phys. Rev. B* **95**, 014413 (2017).
- [21] H. Liu, M. Groesbeck, E. Lafalce, X. Liu, and Z. V. Vardeny, *J. Photonics Energy* **8**, 032212 (2018).
- [22] S. Sanvito, *Nat. Phys.* **6**, 562 (2010).
- [23] M. Cinchetti, V. A. Dediu, and L. E. Hueso, *Nat. Mater.* **16**, 507 (2017).
- [24] V. Coropceanu, J. Cornil, D. A. da Silva Filho, Y. Olivier, R. Silbey, and J.-L. Brédas, *Chem. Rev.* **107**, 926 (2007).
- [25] T. D. Nguyen, G. Hukic-Markosian, F. Wang, L. Wojcik, X. G. Li, E. Ehrenfreund, and Z. V. Vardeny, *Nat. Mater.* **9**, 345 (2010).
- [26] P. A. Bobbert, W. Wagemans, F. W. A. van Oost, B. Koopmans, and M. Wohlgenannt, *Phys. Rev. Lett.* **102**, 156604 (2009).
- [27] Z. G. Yu, *Phys. Rev. Lett.* **106**, 106602 (2011).
- [28] S. Schott, E. R. McNellis, C. B. Nielsen, H.-Y. Chen, S. Watanabe, H. Tanaka, I. McCulloch, K. Takimiya, J. Sinova, and H. Sirringhaus, *Nat. Commun.* **8**, 15200 (2017).
- [29] A. Einstein, *Investigations on the Theory of the Brownian Movement* (Courier Corporation, Berne, 1956).
- [30] Z. G. Yu, *Phys. Rev. Lett.* **111**, 016601 (2013).
- [31] A. Droghetti and S. Sanvito, *Phys. Rev. B* **99**, 094413 (2019).
- [32] H. Liu, C. Zhang, H. Malissa, M. Groesbeck, M. Kavand, R. McLaughlin, S. Jamali, J. Hao, D. Sun, R. A. Davidson, L. Wojcik, J. S. Miller, C. Boehme, and Z. V. Vardeny, *Nat. Mater.* **17**, 308 (2018).
- [33] M. Kavand, C. Zhang, D. Sun, H. Malissa, Z. V. Vardeny, and C. Boehme, *Phys. Rev. B* **95**, 161406(R) (2017).
- [34] R. Miller, K. J. van Schooten, H. Malissa, G. Joshi, S. Jamali, J. M. Lupton, and C. Boehme, *Phys. Rev. B* **94**, 214202 (2016).
- [35] W. J. Baker, T. L. Keevers, J. M. Lupton, D. R. McCamey, and C. Boehme, *Phys. Rev. Lett.* **108**, 267601 (2012).
- [36] D. R. McCamey, H. A. Seipel, S.-Y. Paik, M. J. Walter, N. J. Borys, J. M. Lupton, and C. Boehme, *Nat. Mater.* **7**, 723 (2008).
- [37] H. Malissa, M. Kavand, D. P. Waters, K. J. van Schooten, P. L. Burn, Z. V. Vardeny, B. Saam, J. M. Lupton, and C. Boehme, *Science* **345**, 1487 (2014).
- [38] H. Huebl, F. Hoehne, B. Grolik, A. R. Stegner, M. Stutzmann, and M. S. Brandt, *Phys. Rev. Lett.* **100**, 177602 (2008).
- [39] See Supplemental Material at <http://link.aps.org/supplemental/10.1103/PhysRevLett.124.067702> for extensive details about the electrical device characterization and spin density measurements, which includes Refs. [30,40–42].
- [40] G. R. Eaton, S. S. Eaton, D. P. Barr, and R. T. Weber, *Quantitative EPR* (Springer, Vienna, 2010).
- [41] T. Lanz, E. M. Lindh, and L. Edman, *J. Mater. Chem. C* **5**, 4706 (2017).
- [42] K. Harii, Z. Qiu, T. Iwashita, Y. Kajiwara, K. Uchida, K. Ando, T. An, Y. Fujikawa, and E. Saitoh, *Key Eng. Mater.* **508**, 266 (2012).
- [43] K. Marumoto, N. Arai, H. Goto, M. Kijima, K. Murakami, Y. Tominari, J. Takeya, Y. Shimoi, H. Tanaka, S. I. Kuroda, T. Kaji, T. Nishikawa, T. Takenobu, and Y. Iwasa, *Phys. Rev. B* **83**, 075302 (2011).
- [44] M. Y. Teferi, J. Ogle, G. Joshi, H. Malissa, S. Jamali, D. L. Baird, J. M. Lupton, L. Whittaker Brooks, and C. Boehme, *Phys. Rev. B* **98**, 241201(R) (2018).
- [45] H. Scher and E. W. Montroll, *Phys. Rev. B* **12**, 2455 (1975).
- [46] S.-J. Wang *et al.*, *Nat. Electron.* **2**, 98 (2019).
- [47] Z. G. Yu, *Phys. Rev. B* **85**, 115201 (2012).
- [48] J. Rawson, P. J. Angiolillo, P. R. Frail, I. Goodenough, and M. J. Therien, *J. Phys. Chem. B* **119**, 7681 (2015).
- [49] N. Tombros, C. Jozsa, M. Popinciuc, H. T. Jonkman, and B. J. Van Wees, *Nature (London)* **448**, 571 (2007).
- [50] Y. Fukuma, L. Wang, H. Idzuchi, S. Takahashi, S. Maekawa, and Y. Otani, *Nat. Mater.* **10**, 527 (2011).
- [51] J. Tsurumi, H. Matsui, T. Kubo, R. Häusermann, C. Mitsui, T. Okamoto, S. Watanabe, and J. Takeya, *Nat. Phys.* **13**, 994 (2017).
- [52] E. A. Lukina, A. A. Popov, M. N. Uvarov, E. A. Sutura, E. J. Reijersec, and L. V. Kulik, *Phys. Chem. Chem. Phys.* **18**, 28585 (2016).
- [53] A. Armin, S. Shoaee, Q. Lin, P. Burn, and P. Meredith, *npj Flexible Electron.* **1**, 13 (2017).
- [54] M. Uvarov, J. Behrends, and L. Kulik, *J. Chem. Phys.* **143**, 244314 (2015).
- [55] J. N. Haddock, X. Zhang, B. Domercq, and B. Kippelen, *Org. Electron.* **6**, 182 (2005).
- [56] A. Riminucci, Z. Yu, M. Prezioso, R. Cecchini, I. Bergenti, P. Graziosi, and V. Alek Dediu, *ACS Appl. Mater. Interfaces* **11**, 8319 (2019).
- [57] Y. P. Kandel, H. Qiao, S. Fallahi, G. C. Gardner, M. J. Manfra, and John M. Nichol, *Nature (London)* **573**, 553 (2019).